Journal of Diabetes & Metabolic Disorders (2022) 21:379–397
https://doi.org/10.1007/s40200-022-00985-6

RESEARCH ARTICLE

Integrated omics analysis revealed the *Tinospora cordifolia* intervention modulated multiple signaling pathways in hypertriglyceridemia patients-a pilot clinical trial

Amey Shirolkar[1] · Aarti Yadav[2] · Amit Nale[1] · Jatin Phogat[2] · Rajesh Dabur[1,2]

Received: 8 February 2021 / Accepted: 20 January 2022 / Published online: 1 February 2022

Abstract

Purpose Hypertriglyceridemia (HTG) is strongly associated with the various types of disease conditions and evolving as epidemics. Hence, it is important to identify molecules that lower the triglyceride and chylomicron levels. *Tinospora cordifolia* is an illustrious Ayurveda drug, has proved juvenile and immunomodulatory properties.

Methods Twenty four (24) patients having >499 mg/dL TG and 130–230 mg/dL of cholesterol were randomized and given 100 mL/day (~3.0 g) water extract of *T. cordifolia* (TCE) for 14 days. Basal parameters were analyzed before and after TC intervention to analyzed primary outcomes. Further, unbiased metabolomics and proteomics profiling was explored to assess the efficacy of TCE in HTG patients.

Results TCE intervention decreased the levels of triglycerides, and VLDL to 380.45 ± 17.44, and 31.85 ± 5.88, and increased the HDL levels to 47.50 ± 9.05 mg/dL significantly ($p < 0.05$). Metabolomics analysis identified the significant alteration in 69 metabolites and 72 proteins in plasma of HTG patients. TCE intervention reduced the level of isoprostanes, ROS, BCAA, and fatty acid derivatives, significantly. The annotation databases, Metboanalyst predicted Akt and Rap1 signaling, and ECM-receptor interaction is the most affected in HTG patients. TCE intervention normalized these events by increasing the peroxisome biogenesis and modulating Akt and Rap1 signaling pathway.

Conclusion *T. cordifolia* intervention suppresses the baseline in HTG patients. Omics analysis showed that TCE intervention modulates the Akt and Rap signaling, and peroxisome biogenesis to control the cellular switches and signaling pathways. Hence, TCE can be used as a supplement or alternate of standard drugs being used in the management of HTG.

Keywords Hyperlipidemia · Hypertriglyceridemia · *Tinospora cordifolia* · HPLC-ESI-QTOF-MS · 2-dimensional gel electrophoresis

Introduction

Hypertriglyceridemia (HTG) is characterized by isolated elevation of triglycerides, VLDL (very low-density lipoprotein) and LDL (low-density lipoprotein) particles, and low count of HDL (high-density lipoproteins). It is asymptomatic by nature, hence often observed after the development of onsets of problems [1]. Its silent etiology is a milieu of various metabolic disorders, obesity, acute pancreatitis, atherosclerosis, non-alcoholic fatty liver, and cardiovascular diseases (CVDs). Moreover, it may be secondary in insulin resistance, obesity, alcohol abuse, chronic kidney disease, and several endocrinal diseases [2–4]. Obesity is now epidemic, hence the frequency of

Amey Shirolkar and Aarti Yadav contributed equally to the research work discussed in the research article, hence both should be treated as first authors.

✉ Rajesh Dabur
rajeshdabur@yahoo.com

[1] Department of Biochemistry, National Research Institute of Basic Ayurvedic Sciences (NRIBAS), Kothrud, Pune, Maharashtra 411038, India

[2] Department of Biochemistry, Maharshi Dayanand University, Rohtak, Haryana 124001, India

HTG will rise being concurrent metabolic syndrome of obesity [4]. It has been reported that hypertriglyceridemia contributes to 10% of acute pancreatitis and 30% to insulin resistance [5–7]. Despite all efforts, the exact mechanism behind the HTG is not fully understood.

Major drugs being used are fibrates and statins [7]. Fibrates modulate peroxisome proliferator-activated receptor-α (PPAR- α) that decreases the triglyceride concentration by 50%, however, it also increases the LDL-C up to ~20%, a major risk factor of CVDs [8]. The second class of drugs i.e. statins inhibit the activity of 3-hydroxy-3-methylglutaryl-coenzyme A reductase, hence these are not the first-line therapy for HTG [9]. Other HTG therapies involve niacin and bile acid-binding resins to increase lipid catabolism and reduce intestinal absorbance of lipid, respectively [10] . More focus is now on the therapies which decrease the ApoB levels rather than LDL-C. Hence, statins with cholesteryl ester transfer protein (CETP) inhibitors are found to be more useful to decrease apoB levels without any change in LDL-C and HDL-C [10, 11]. Hence, present drugs alone are not sufficient to control triglyceride levels in HT patients and need extra managements like diet and exercise control. Moreover, even after successful management of HTG, residual CVD risk is always there. Therefore need to identify a novel drug that suppresses the remnants of chylomicron and to counteract the progressive accumulation of triglycerides.

Tinospora cordifolia (TC) (Willd) Miers is a large, deciduous, climbing shrub belongs to Menispermaceae family and commonly known as s*angrahi,* guduchi, *amrita, etc* [10]. *Ayurveda, an ancient Indian system of medicine prescribed the use of T. cordifolia in form of its water extract (TCE), decoction, and other formulations alone and with other herbal drugs. T. cordifolia accommodates numerous bioactive compounds such as alkaloid, flavonoids,* glycosides, tannins, terpenoids, and coumarins [12, 13]. *It was reported to attribute as anti-inflammatory, anti-oxidative, anti-diabetic, anti-arthritis, hypoglycemic,* hypolipidemic, and anti-allergic [14, 15]. TC intervention was reported to attenuate the accumulation of thiobarbituric acid reactive substances (TBARS) and restored insulin sensitivity in T2DM rats [15]. Another study showed that TC suppressed the release of pro-inflammatory cytokine in arthritis individuals through inhibition of NF-kB [16]. Moreover, TC supplementation supported the β-oxidation and reduces the triglycerides level [17]. Berberine is well studied alkaloid has proved efficacy in hyperlipidemia [18] that could not enter in clinical trials due to high toxicity [19]. In TCE several protoberberines alkaloids including palmatine and magnoflorine are present in significant amounts have in vitro efficacy to treat metabolic disorders [12]. Therefore, based on its multi-regulatory efficacy, TCE might act as potent therapeutic agent to suppress the HTG and its associated complication. Hence, the purpose of the present randomized pilot clinical trial was to evaluate the efficacy of TCE in HTG and to delineate its mechanism.

Materials and methods

Chemicals & reagents Routine biochemical assays were carried out using commercial kits obtained from Erba Mannheim kits (Lot) (TG-B111817; Total Cholesterol-S111927; ALT, BLT00052; AST-BLT00050; Creatinine-E111229; Glucose-S111909; Total protein-BLT00054; Albumin-BLT00001, Uric acid-BLT00062; Haemoglobin- BLT20020. HDL and VLDL/LDL(ab65390) assay kit procured from Abcam, USA. Internal and external calibrants and ESI tuning solution were purchased from Agilent Technologies. Standards of amino acids and metabolic markers were purchased from Sigma (St. Louis, MO). HPLC grade solvents and reagents used in experimentation like acetonitrile, methanol, formic acid, water, isopropanol, glacial acetic acid, and Bradford reagent were purchased from Sigma (St. Louis, MO). Immobiline dry strips (IPG, pH 3–10, 18 cm), DeStreak™ rehydration solution and pharmalyte (pH 3–10), Mineral oil were procured from GE Healthcare, acrylamide, bisacrylamide, SDS, urea, bromophenol blue, DTT, agarose, iodoacetamide, glycerol, tris base, ammonium persulfate, glycine, TEMED, silver nitrate, formaldehyde, sodium carbonate, sodium thiosulfate were of molecular biology/ analytical grade.

Ethical clearance The present clinical trial was approved by the Human Ethics Committee of the PDDYP Ayurveda College, Pune, India wide letter no. RRI/2011/HEC/2023 dated 18-02-2011. This random trial was registered with the Clinical Trials Registry - India (CTRI) wide registration number CTRI/2016/08/007187. All the protocols approved by the ethical committee were as per guidelines of the *Indian* Council of Medical Research (ICMR), *India and no deviation has been made in the protocol while doing experimentation.*

Drug preparation *T. cordifolia* (Willd) Miers stems were collected in September month from the garden of NRIBAS voucher specimens (No. 207), Kothrud, Pune, India. After washing in tap water the stems were crushed and extracted with distilled water overnight at room temperature (1:5 w/v). The extract was filtered and centrifuged at 5000 rpm. The fresh extracts were given to the volunteers to avoid the degradation of Phyto-constituents [20]. Random extracts were subjected to LC-MS analysis for quality control purposes.

Study design The study design, sample collection, data processing, and data analysis opted for current study is listed

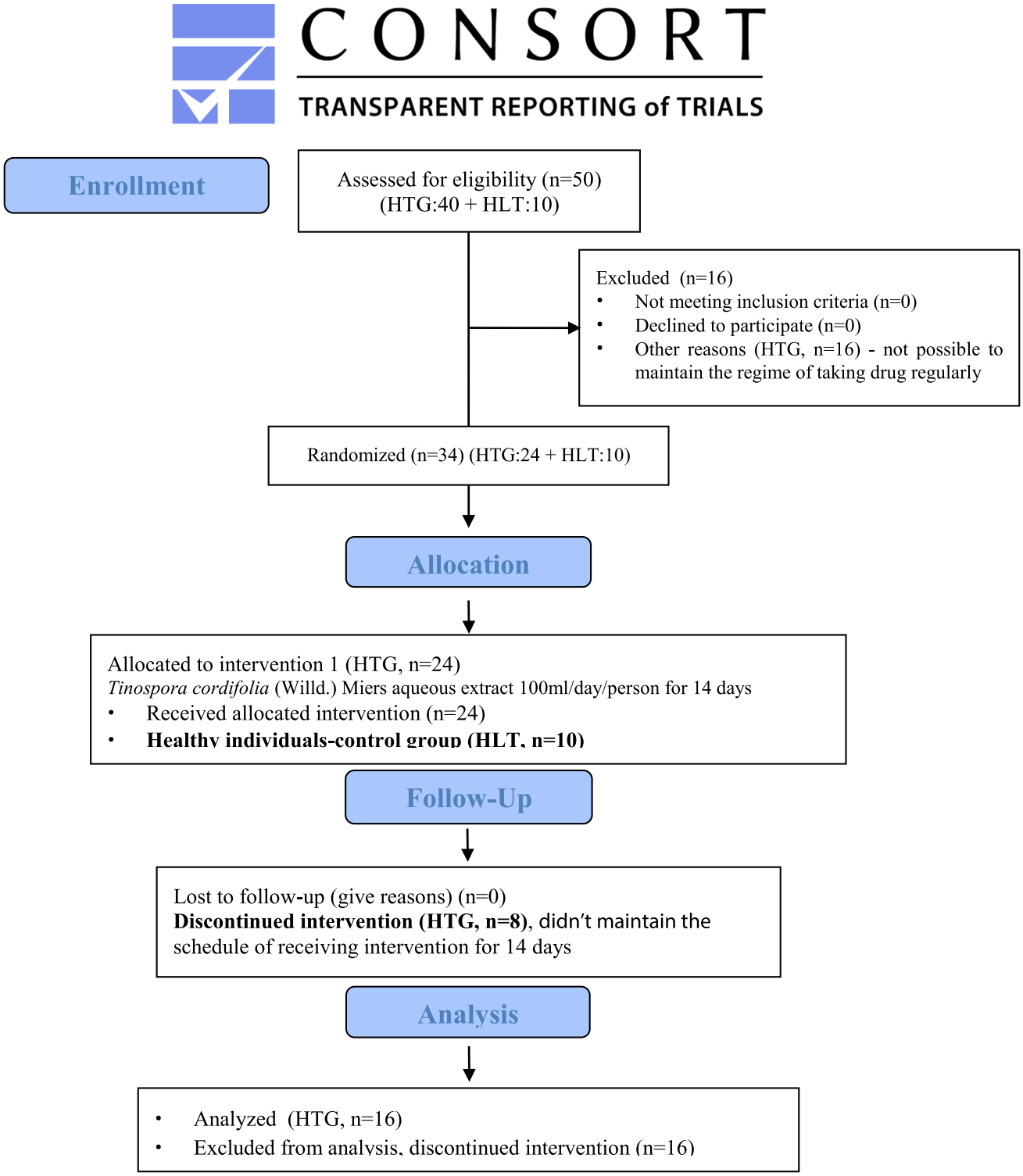

Fig. 1 A CONSORT flow diagram of study design, sample collection, data processing, and data analysis in different study groups

in Fig. 1. Male volunteers were randomly assigned based on their TG levels. Normal individuals serve as the control groups (n = 10). The individual having TG levels more than 499 mg/dL and completed the criteria serve as the HTG group (n = 24). All individuals were consigned to follow the normal diet routine of breakfast, lunch, and dinner with 2 cups of tea in the day time during the trial. After the baseline assessment, HLT and HTG groups were treated with

TCE and assigned as healthy treated with TCE (HLT_T) and HTG treated with TCE (HTG_T). Individuals who able to maintain the regime of TG level [21, 22] has been included in the study. While individuals having prior history of diabetes mellitus, alcoholic, autoimmune, reproductive disorder etc. were excluded from the study. The sample sizes were calculated using Gpower analysis 3.1. The randomized block container method has been used to equally allocate the individuals to decrease the inconsistency among the groups. An Ayurveda physician recruited the random allocation through numbered containers and masked the sequence until intervention was distributed.

Both healthy individuals and HTG patients received 100 mL extract (~3.0 g. solid extract) in the morning before breakfast for 14 days with pre and post follow up phase. In contrast, 16 individuals were unable to maintain the regime of treatment and excluded from the study. Fasting blood has been collected on day 0 and day 14 in K^+-EDTA vials, centrifuged and collected plasma samples were stored at −80 °C for further use. Aspirated plasma fraction was subjected to assess baseline parameters. The preliminary efficacy of TCE was evaluated through the change in TG, TC, VLDL, LDL, HDL, AST, ALT, etc. on day 0 and day 14 via autoanalyzer (ERBA, Germany) and blood cell counter using Erba Mannheim kits and GRA H360 Hematology Analyzer. While secondary outcomes were characterized through the identification of oxidative stress markers, altered metabolic pathways, proteomics study and to generate the interlinking bridge between the altered markers and signaling event.

HPLC Qualitative and quantitative metabolomics experiments were performed on Agilent 1290 Infinity Series HPLC interfaced to an Agilent 6538 Accurate-Mass Q-TOF MS. Plasma samples were diluted with acetonitrile: water (80:20 v/v) in 1:4 ratio and centrifuged at 8000 rpm for 5 min at 15 °C [17]. The volume of 20 µL of each sample was injected into an assembly of the C18 ZORBAX (4.6 × 12.5 mm) guard column followed by ZORBAX 300SB-C18 (4.6 × 150 mm) column of particle size 5.0 µm. The column temperature was set at 40 °C and that of the autosampler was 5 °C. The solvent system (A) had aqueous, 0.1% formic acid - water, and (B) organic, 0.1% formic acid - acetonitrile in the proportion of 90:10. The gradient mode {concentration/time (%/min)} used for solvent B was 0%/0; 100%/30; 0%/42; 0%/50}, with 0.5 mL/min flow rate. The mass spectrometer was operated in positive ion polarity mode with parameters: electrospray ionization (ESI), gas temperature 350 °C, nebulizer 50 psi, gas flow 12 l/min, capillary voltage 3500 V, nozzle 750 V, and fragmentor voltage 195 V. The data acquisition was carried out in the range of 100–1200 m/z. The quadrupole was operated in the extended dynamic range (1700 m/z, 2GHz).

Quality control of the data To ensure the mass accuracy of recorded data, continuous internal calibration was performed using standards of signals of standard compounds. Pooled samples from the different groups were also used for quality control purposes. Blank samples (a solvent mixture of acetonitrile and water) were also injected between the sample runs. The chromatograms of blank samples were used to study the carry-over effects in LC-MS runs.

Multivariate analysis Mass Hunter Qualitative Analysis (B.04.00, Agilent Technologies) software was used for preliminary investigation of raw MS/MS data such as correction, noise reduction, background removal, contaminants, and extraction of molecular features. Molecular features having >5000 cycles per second (cps), minimum absolute counts 10, relative height (5%) of largest peak, peak space tolerance, i.e. 0.0025 m/z, and 5.0 ppm were extracted from mass spectra to avoid false molecular features.

Quantitative analysis of selected molecular markers To support qualitative analysis, a set of 45 metabolic markers and nine isoprostanes (IsoPs) were analyzed quantitatively in targeted MS/MS mode (SRM-selective reaction monitoring). HPLC-QTOF-MS conditions for quantitative analysis were similar to qualitative metabolomics studies except for collision energies. Collision energy for each metabolite was kept as suggested by [23]. The standard curves of standards were prepared in a range of 0.09 to 50 µg/mL. Various metabolites in plasma were quantified with help of their standards using Quantitative Analysis software (version B.04.00) from Agilent Technologies from the area ratio of the peaks. Concentrations of metabolites in plasma samples were analyzed using a standard curve with the highest correlation coefficient ($R^2 \geq 0.95$). A signal-to-noise ratio (SNR) threshold of >3.0 was used. The limit of detection (LOD/ qualifier) and limit of quantitation (LOQ/quantifier) values were calculated based on the reported formulae, LOD = 2 N/m, where N is the noise value in SNR and m is the slope in peak height v/s concentration plot; LOQ = 5 x LOD.

Depletion of abundant proteins and protein quantitation Prior proteomic studies the albumin; globulin and other abundant proteins were removed from plasma samples by using a kit from Calbiochem and according to the manufacturer instructions. The total protein concentrations of whole and depleted plasma samples were determined using the Bradford assay kit (Sigma) and bovine serum albumin (BSA) as the standard (A_{595}).

2-dimensional gel electrophoresis For the isoelectric focusing (IEF, first dimension) sample containing 40 µg of protein were mixed in DeStreak ™ solution (340 µL) containing optimized concentrations of urea, thiourea, CHAPS, and

bromophenol blue (BPB). The samples were applied on an 18 cm IPG strip covering a pH range of 4–7 and rehydrated for 20 h. Rehydrated IPG strips were subjected to Ettan IPGphor 3 system (GE Healthcare). For the separation appropriate time and voltage profile were used: 500 V for 1 h, 1000 V for 1 h gradient, 8000 V for 4 h gradient, and 8000 V for 2 h to attain 35,250 Vhs of potential difference in 8 h. Focussed IPG strip was subjected to equilibration with buffer I (GE Healthcare) containing SDS, urea, glycerol, and DTT for 15 min. IPG strips again equilibrated in the buffer II where DTT was replaced with iodoacetamide for another 15 min. After equilibration, focussed strips were placed on top of each gel (12.5%) of Ettan DALT six systems and sealed with 1% of agarose solution along with protein marker (3.5–434 kDa, Genei). A current of 100 mA was applied for the first hour and then 150 mA was applied till the bromophenol blue dye front reached the anodic end (+). Three replicate gels were run for each of the plasma samples to further cut-down the gel-to-gel variation and handling errors.

The electrophoresed protein gels were silver stained according to the protocol described by [24]. Computerized 2-D gel analysis was performed using Melanie powered Image Master 2D Platinum software (GE Healthcare). All gels in parallel compared in this software as HTG_T vs HLT and HTG_T vs HTG. Few most repeated spots were first labeled as landmarks and then class and match sets were made, all spots were labeled. The analysis included creating match sets of HTG vs HLT and HTG_T vs HTG for gel images, detecting spots, and creating classes. ANOVA ($p < 0.05$) test was applied over the sampling class to obtain the statistically significant differentially expressed protein spots. The 3D view was obtained for these spots to mark the effect of treatment on the level of proteins. Spot intensity parameter was used for discriminating proteins as up or downregulated in classes of comparison. Differentially expressed protein spots were excised from gels and transferred into fresh vials for trypsin digestion. Tryptic digestions of differential protein spots were performed using the in-gel trypsin digestion kit (Calbiochem) following the supplier's instructions. In brief, excised protein spots were de-stained, dehydrated, reduced with DTT, alkylated with iodoacetamide, and digested overnight at 37 °C in the presence of trypsin. The reaction was quenched with formic acid and reaction volume was transferred to sampling vials into autosampler.

Identification of differential proteins For protein identification, HPLC-QToF-MS experiments were performed on Agilent 1290 Infinity Series HPLC interfaced with an Agilent 6538 Accurate-Mass Q-TOF MS. A volume of 20 µL of each sample was injected into an assembly of C18 ZORBAX 300 extend (4.6 × 150 mm) column of particle size 3.5 µm. The column temperature was set at 40 °C and 5 °C of the autosampler. The solvent system had aqueous (A), 0.1% formic acid-water, and organic (B), 0.1% formic acid-acetonitrile in the proportion of 95:5. The gradient mode {concentration/time (%/ min)} used for solvent B was 3%/0; 60%/10; 97%/14; 97%/15.5; 30%/21; 5%/25; and 5% at 30 min with 0.3 mL/min flow rate. The mass spectrometer was operated in positive ion polarity mode with parameters: ionization type dual electrospray ionization (ESI), gas temperature 325 °C, nebulizer 45 psi, gas flow 9.0 l/min, capillary voltage 3500 V, nozzle 750 V, and fragmentor voltage 150 V. The data acquisition was carried out in the range of 100–3000 m/z. The quadrupole was operated in the extended dynamic range (1700 m/z, 2GHz). The data was stored in profile mode that corresponds to continuous data storage. Protein identification was performed with the spectrum mill database search tool (A.03.03, Agilent Technologies). Obtained MS/MS spectrums were searched against the *Homo sapiens* NCBI database. The searches were run using the fixed modification of carbamidomethylation labeled cysteine and methionine oxidation as a variable modification parameter. Other parameters were set as MS spectral features, $M + H^+$ 600 to 60,000 m/z, extraction time range 0 to 30 min., a loud charge states 2–4, maximum ambiguous precursor charge 3, precursor mass tolerance ±1.0 Da, product mass tolerance ±0.5 Da, maximum missed cleavages 4, minimum detected peaks 4, sequence tag length > 3, protein pI 3.0–10.0 and maximum reported hits 5. After validation, a summary of peptides was obtained from a single protein spot. This data was further confirmed using the deconvolution tool (Bioconfirm) in the MassHunter (Agilent) to calculate the actual molecular mass of the proteins from the concerned mass data files.

Statistical analysis Power and sample size was calculated using Gpower analysis 3.1. having sample size (n = 24), the size effect of 0.4677, significance level ($\alpha > 0.05$), and 80% of statistical power were used to evaluate the potential of TCE. In the present randomized trial, basal parameters were represented as mean ± SD analyzed using GraphPad Prism 7 to evaluate the potential of TCE in healthy and HTG individuals.

For metabolomics data analysis mass profiles were imported in Mass Profiler Professional software (B.12.02, Agilent Technologies) and all the molecular features were aligned using mass error < 5.0 ppm and retention time (RT) variation <0.2 min. Compounds present in less than 75% of samples of a group and having $p > 0.05$, fold change <2.0, and coefficient of variance <15 were removed from data sets and subjected to principal component analysis (PCA). Box-Whisker plot was also generated to analyze the distribution of data segregated under different categories. Finally, partial least-squares-discriminant analysis (PLS-DA) was

performed to distinguish different groups and explore unique features present across the groups. Data obtained were further subjected to Wilcoxon paired t-test, One way ANOVA with Bonferroni multiple testing corrections to minimize the false discovery rate, keeping up p value cut off <0.05 and fold change >2.0. Differential metabolites were identified by comparing the fragmentation pattern of the metabolites with the standards in Metlin, HMDB, NIST databases, and literature.

Database for Annotation, Visualization, and Integrated Discovery (DAVID) version 6.8, online software was used to explore biological processes and signaling pathways associated with proteome data. Cytoscape 3.8.0 and MetaboAnalyst (statistical, functional, and integrative analysis of metabolomics and proteomics data) were used to explore various pathways alerted in HTG and HTG_T groups.

Results

Characterization of TCE The optimized solvent system for HPLC and QTOF-MS parameters to resolve and identify the TC constitutes in TCE were described earlier [20]. The chromatograms of blank samples contained only low-intensity peaks, hence it was concluded that the carry-over effect did not occur. The LC-MS analysis of TCE was also carried out in comparison to solvent blanks. The TCE (drug) showed great repeatability and had many prominent peaks that corresponded to *Tinospora* specific compounds such as magnoflorine, palmatine, etc. The composition of TCE and quality control for the extracts used in this study has already been reported [17] 12]. TCE was found to be enriched in alkaloids namely magnoflorine, palmatine, and some other compounds.

Clinical biochemistry Basal parameters including TG, VLDL, LDL, HDL, AST, ALT, etc. revealed a significant difference in TCE treated group. In the HTG_T group, the TG level was depleted significantly ($p < 0.05$). Likewise, decreased levels of LDL and increased levels of HDL were observed in HTG_T group. Levels of uric acid were also reduced significantly after treatment with TCE. The ALT/AST ratio was observed to be higher in HTG as compared to HLT group. The decrease in the activity of AST along with ALT/AST ratio was also observed in the healthy group as well in TCE treated healthy group. TCE supplementation had also reduced the levels of urea, creatinine, albumin and glucose in HTG pateints. TCE treatment reduced glucose levels but enhanced the Hb%, number of RBCs, and platelets in both HTG_T as well in HLT_T groups (Table 1).

Table 1 The blood biochemistry, lipid profiles and *hematocrit* of all the groups employed in the study are expressed as mean ± SD ($p < 0.05$). BMI: Body Mass Index; TG: Triglycerides; TC: Total Cholesterol; HDL: High Density Lipoprotein; LDL: Low Density Lipoprotein; VLDL: Very Low-Density Lipoprotein; AST: Aspartate transaminase; ALT: Alanine transaminase; RBCs: Red Blood Cells; WBCs: White Blood Cells

S No	Parameters	Healthy Individuals		Hypertriglycedemic patients		*p* value
		HLT (Day 0)	HLT_T (Day 14)	HTG (Day 0)	HTG_T (Day 14)	
1.	Age (years)	39.2 ± 2.4	39.2 ± 2.4	39.4 ± 1.6	39.3 ± 1.4	ns
2.	BMI	22.1 ± 2.2	22.9 ± 1.5	25.6 ± 2.1	24.08 ± 1.9	0.006426
3.	TG (mg/dL)	98.36 ± 3.0	85.20 ± 4.30	550.00 ± 18.5	380.45 ± 17.4	< 0.0001
4.	TC (mg/dL)	155.13 ± 4.4	140.20 ± 4.5	167.26 ± 6.0	160.55 ± 3.3	< 0.0001
5.	HDL (mg/dL)	45.10 ± 2.5	48.66 ± 5.8	35.50 ± 6.5	47.50 ± 9.0	< 0.0001
6.	LDL (mg/dL)	108.50 ± 6.1	99.73 ± 3.1	157.91 ± 11.1	133.25 ± 3.1	< 0.0001
7.	VLDL	18.26 ± 3.6	14.65 ± 2.8	69.56 ± 5.6	31.85 ± 5.8	< 0.0001
8.	Urea (mg/dL)	17.56 ± 8.9	16.10 ± 4.0	30.26 ± 1.7	27.60 ± 5.9	< 0.0001
9.	Creatinine (mg/dL)	0.89 ± 0.6	0.83 ± 0.4	1.35 ± 0.4	0.95 ± 0.0	< 0.0001
10.	Total Protein (g/dL)	5.6 ± 0.3	6.3 ± 0.3	5.35 ± 0.4	5.0 ± 0.5	0.00066
11.	Albumin (g/dL)	4.06 ± 0.4	3.30 ± 2.0	5.20 ± 0.1	3.90 ± 1.2	0.00002
12.	ALT (U/L)	21.46 ± 2.2	21.06 ± 6.5	36.05 ± 6.3	24.95 ± 4.0	< 0.0001
13.	AST (IU/L)	27.10 ± 3.6	18.96 ± 7.5	23.45 ± 4.2	20.55 ± 6.3	< 0.0001
14.	Uric acid (mg/dL)	4.93 ± 0.9	4.16 ± 0.6	7.10 ± 0.9	5.15 ± 0.9	0.000277
15.	Glucose (mg/dL)	97.06 ± 7.0	85.16 ± 6.5	105.95 ± 8.5	102.05 ± 7.8	0.000203
16.	Hemoglobin % (g/dL)	13.63 ± 1.6	14.90 ± 1.7	12.65 ± 1.3	14.25 ± 0.6	0.003895
17.	RBCs ($\times 10^6$)	4.79 ± 0.3	5.23 ± 0.1	4.66 ± 0.6	5.06 ± 0.0	0.081382
18.	WBCs ($\times 10^3$)	7.35 ± 1.0	6.48 ± 1.2	7.95 ± 0.3	7.35 ± 1.7	0.02267
19.	Platelets ($\times 10^3$)	296.40 ± 12.3	313.60 ± 8.2	276.50 ± 9.4	342.50 ± 4.7	< 0.0001

*ns = not significant

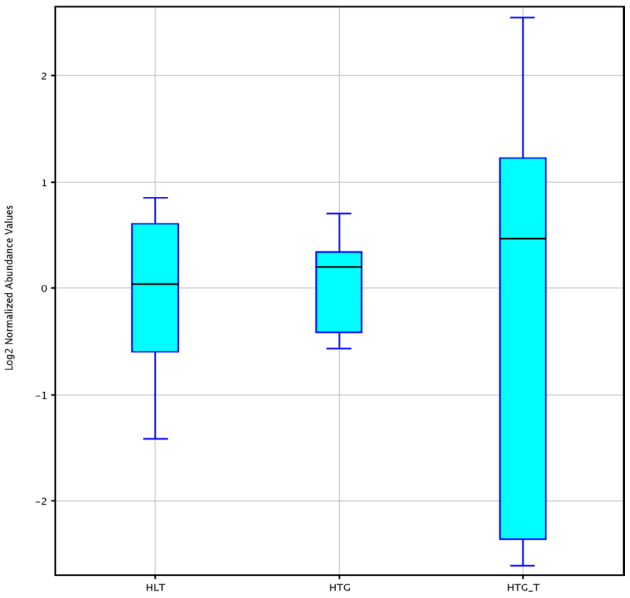

Fig. 2 The box-and-whisker plot reflecting the distribution of metabolites in healthy (HLT), hypertriglyceridemic (HTG) and *T. cordifolia* treated hypertriglyceridemic (HTG_T) patients

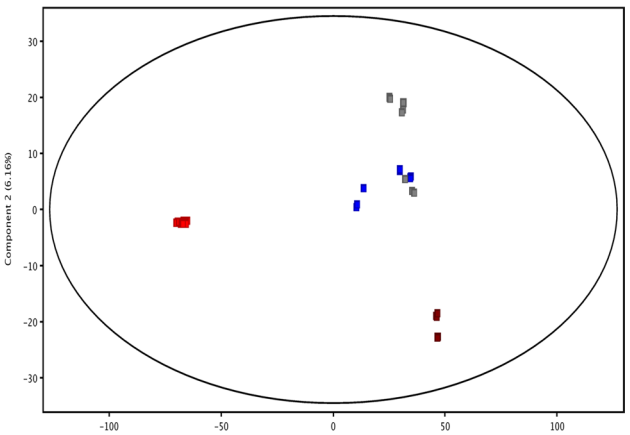

Fig. 3 PCA plots of variable metabolites obtained in positive mode showed significant differences among groups. X axis component value was 36.2% while for Y and Z it was 21.3%, 9.5% respectively. indicates healthy (HLT) population, indicates HLT_T treated, indicates HTG individuals, indicates HTG_T individuals

Multivariate analysis of plasma metabolome Analysis of total ion chromatograms showed an average of 73 peaks containing around 1050 compounds. The analysis method was optimized and the results were reproducible with minimum variations across the samples. Variability in the higher peaks was normalized successfully using internal standards and Z-transforms. The overall percent variance was represented as a box-whisker plot showing altered metabolites as well proteomics across all groups, i.e. HLT, HTG, and HTG_T (Figs. 2, 3, 4, and 5). Out of these, HTG_T showed the highest compound variability represented by elongated box shapes towards either side to the grand mean. Further to explore the clustering in different groups, the molecular features sorted out from different groups after treatments showed a shift of HTG_T group toward healthy controls. Supervised PCA of HLT, HTG, and HTG_T groups showed 47.55%, 20.54%, and 5.22% variability along the X, Y, and Z axes respectively (Fig. 3). However, variability between TCE treated and healthy decreased significantly. To refine data further and to identify major changes in molecular features, in partial least square discrimination analysis (PLS-DA) and support vector machines (SVMs) to support the satisfactory model for LC-MS ($R^2 = 0.97$ and $Q^2 = 0.86$). Hence, the results from PLS-DA and SVM are showing consistency with PCA observations and high accuracy of models. These results showed clear differences among groups and maximum metabolites perturbation in HTG patients.

Qualitative analysis and identification of variable metabolites Data from SVM was further processed performing Mann-Whitney U-test with 50 permutations and Bonferroni FWER multiple testing corrections to remove false molecular features. Moreover, the metabolites with any missing values were filtered out. Finally, 69 molecular features with variable importance on projection (VIP) values >1.5 and $p < 0.05$ were identified (Table 2). These metabolites were identified using their corresponding MS/MS spectra and matching them with different databases. These 69 metabolites broadly can be divided into lipids, haems, vitamins, bile acids, nucleotides, amino acids, and oxidative stress markers and are presented in Table 2. For example, most of the lipids were identified as phospholipids and observed to be increased in the HTG group as compared to HLT, and decreased after TCE intervention in the HTG group. Bile acid intermediates i.e. 4α-formyl-5α-cholesta-8, 24-dien-3β-ol, and 3α, 7α-dihydroxy-5β-cholestane, intermediates in bile acid synthesis and nutriacholic acid was observed to be upregulated in HTG group (FC > 2.0) and down-regulated after TCE intervention (Table 2). Similarly, vitamins i.e. folic acid, nicotinic acid, α-tocopherol acetate, 2-oxo-3-hydroxy-4-phosphobutanoic acid, and thiamine monophosphate showed a common decreased trend in the HTG group in comparison to HLT and increased levels in the HTG_T group (Table 2).

Oxidative burden measurement Isoprostanes (IsoPs) are the products of arachidonic acid due to enzymatic or non-enzymatic actions. These are the best markers of oxidative stress as well as inflammation. Hence**,** IsoPs levels in the plasma samples from all groups were analyzed using selective ion monitoring method with predetermined LC-MS parameters including fixed collision energy (eV) in both positive and negative modes of ion polarities (Table 3).

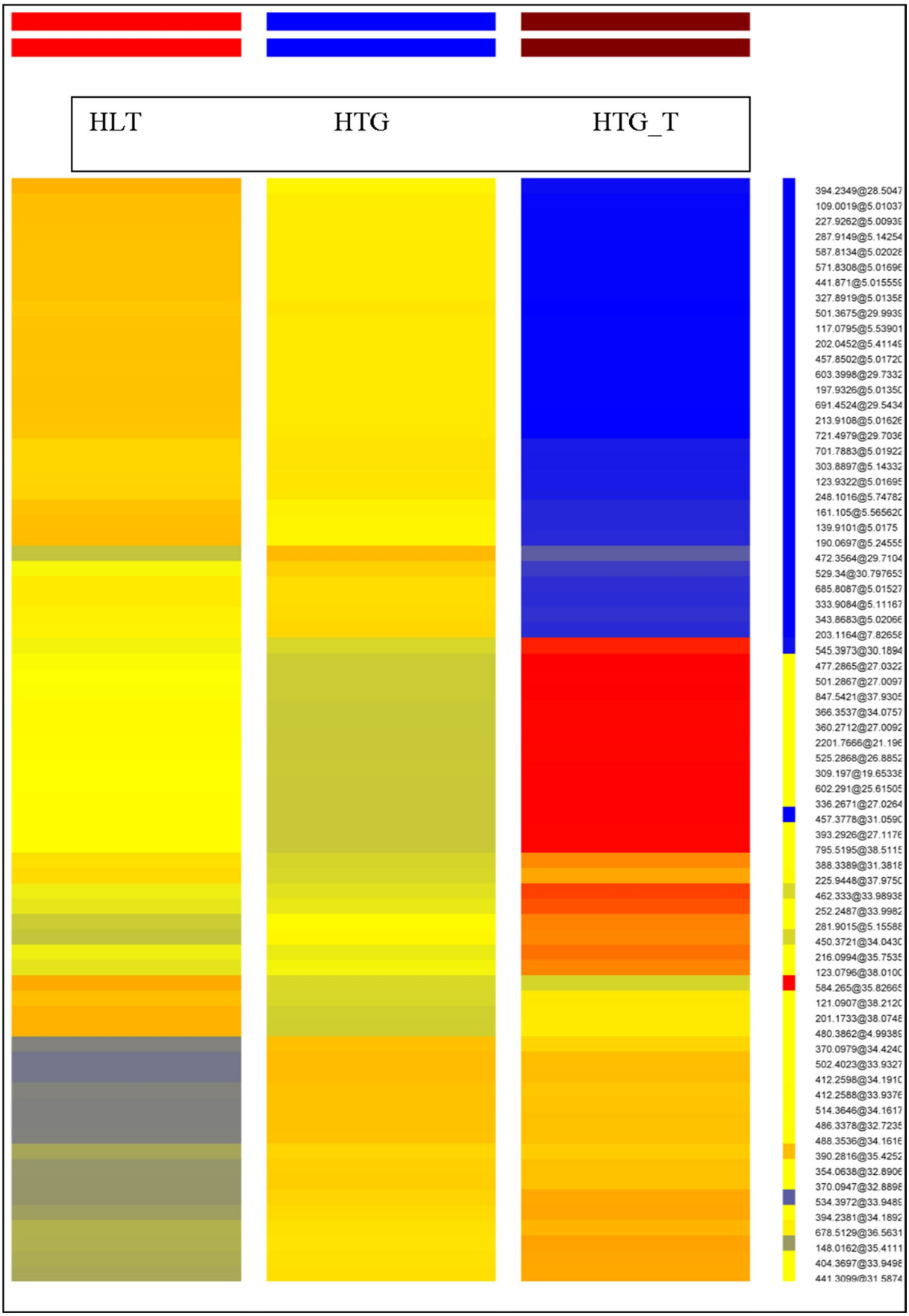
HLT
HTG
HTG_T
394.2349@28.5047
109.0019@5.01037
227.9262@5.0093
287.9149@5.14254
587.8134@5.0202
571.8308@5.0169
441.871@5.01555
327.8919@5.0135
501.3675@29.993
117.0795@5.53901
202.0452@5.4114
457.8502@5.0172
603.3998@29.733
197.9326@5.0135
691.4524@29.5434
213.9108@5.0162
721.4979@29.703
701.7883@5.01922
303.8897@5.1433
123.9322@5.0169
248.1016@5.74782
161.105@5.56562
139.9101@5.0175
190.0697@5.2455
472.3564@29.7104
529.34@30.79765
685.8087@5.01527
333.9084@5.11167
343.8683@5.0206
203.1164@7.8265
545.3973@30.1894
477.2865@27.0322
501.2867@27.0097
847.5421@37.930
366.3537@34.0757
360.2712@27.0092
2201.7666@21.19
525.2868@26.8852
309.197@19.6533
602.291@25.6150
336.2671@27.0264
457.3778@31.059
393.2926@27.117
795.5195@38.511
388.3389@31.381
225.9448@37.975
462.333@33.9893
252.2487@33.9982
281.9015@5.1558
450.3721@34.043
216.0994@35.753
123.0796@38.010
584.265@35.8266
121.0907@38.212
201.1733@38.074
480.3862@4.9938
370.0979@34.424
502.4023@33.9327
412.2598@34.191
412.2588@33.937
514.3646@34.1617
486.3378@32.723
488.3536@34.161
390.2816@35.4252
354.0638@32.890
370.0947@32.889
534.3972@33.948
394.2381@34.1892
678.5129@36.5631
148.0162@35.4111
404.3697@33.949
441.3099@31.5874

◂**Fig. 4** Pearson heat map alignment of differential metabolites across healthy (HLT), hypertriglyceridemic (HTG), and TCE-treated HTG (HTG_T) groups. The columns correspond to different individual groups and rows correspond to the altered metabolites

The average LOD and LOQ for IsoPs were in the range of 0.146 and 0.734 µg/mL respectively with ≥0.95 correlation coefficient (R^2) in both ionic modes (Table S3). *8*-iPGF2α and *8*-iso-*iPGE2* have a major role to stimulate vasoconstriction and proliferation of vascular smooth muscles. In the present study it was observed that the levels of most of the IsoPs were increased (about 1.5 to −3.0 folds, $p < 0.001$) in the HTG patients compared to control and it reverted to normal or below normal upon treatment with TCE in the HTG_T group (Table 3).

Quantitation of other metabolites The LOD and LOQ values, retention time, the precursor to product transition, correlation coefficient (R^2), collision energy of 45 metabolites have been recorded. The average LOD and LOQ for markers were 2.6 and 12.9 µg/mL respectively with ≥0.95 correlation coefficient (R^2) in both ionic modes (Table S2). Out of 45, arachidonic acid, bilirubin, cysteine glycine, DL-homocysteine, and linoleic acid were analyzed in positive as well as the negative mode of ion polarity. Overall, 4 types of trends were observed, i.e. higher concentration in HTG than HLT get reduced in HTG_T; higher concentration in HTG than HLT get increased further in HTG_T; lower in HTG than HLT get increased after TCE treatment; and lower in HTG than HLT get reduced further after TCE treatment (Table 4).

Unbiased proteome analysis As a result of thorough standardization attempts and controlled variables a great extent of repeatability and resolution was observed in 2D protein gels (Fig. S2). The variations in protein spot intensities would be the most basic criteria of comparison of changes in protein expression hence spot intensities of some major proteins within HTG vs HLT and HTG_T vs HTG were compared. A total of 757 match identities were allotted to the protein spots. The factor projection plot of HTG vs HLT comparison displayed the projection and contribution of each match and each gel (blue vector) on the two factorial axes. It measures if the projection of the match is well represented on the factorial subspace. In HTG vs HLT comparison, 65 proteins were analyzed, out of them, 46 were down-regulated and the rest were found upregulated (Table 5). HTG_T vs HTG comparison had 88 proteins, among 39 were down-regulated and 49 were upregulated (Table 6). Differentially expressed proteins were subjected to in-gel digestion and Q-TOF-MS. Data obtained were imported in the Spectrum mill, a database search tool provided probable identification of differentially expressed proteins.

Pathway analysis Cytoscape 3.8.0 plugin MetScape and MetaboAnalyst (statistical, functional, and integrative analysis of metabolomics data) analysis of metabolomics data showed the significant alteration in thiamine, glycerophospholipid, taurine, and nicotinamide metabolism (Table S4). Quantitative analysis confirmed the alterations in the metabolic pathways along with increased oxidative stress. Moreover, the quantitative analysis also showed alterations in arginine, BCCA, aromatic amino acids, and pantothenate biosynthesis and glutathione, linoleic acid, and thiamine metabolism. The Functional annotation chart obtained through DAVID suggested down-regulated PI3K-Akt and Rap1 signaling pathway, decreased ECM-receptor interaction, and increased protein digestion in hypertriglyceridemia patients. TCE supplementation modulated both signaling pathways through activation of peroxisome biogenesis and increasing the synthesis of ECM proteins including actin and tubulin (Table S5). Final pathways were analysed using Cluego plugin Cytoscape 3.8.0 plugin (Fig. 6).

Integrated omics analysis Integrated analysis of metabolomics and proteomics outcome through Cytoscape 3.8.2 plugin Metscape and Metaboanalyst revealed that hypertriglyceridemia altered the protein digestion, HIF-1 signaling pathway, AGE-RAGE signaling, Rap1, PI3K-Akt signaling, and ECM remodeling (Table S6).

Discussion

In the present clinical trial, a two-week treatment with TCE significantly ($p < 0.05$) reduced the basal albumin, TG and VLDL levels and increased the HDL, RBC, and platelet levels ($p < 0.05$) in HTG patients. Decresed in level of albumin is further supported by Sun et al., 2020 after fenofibrate treatment [25]. TCE intervention also reduced the levels of total proteins, creatinine, uric acid, and urea significantly ($p < 0.05$) (Table 1). The efficacy data are consistent with the reports from previous studies [26]. Moreover, the healthy individual didn't show any kind of toxicity symptoms and maintained all the basal parameters at normal levels after the 14th day of treatment. Likewise, a slight increase in HDL, RBCs, and platelets indicated the beneficial effects of TCE in healthy individuals (Table 1). Hence, the primary outcomes of the pilot clinical trial illustrate the beneficial effects of TCE intervention in HTG patients.

Metabolomics profiles indicated that the protein, glutathione, taurine and hypotaurine metabolism, ferroptosis, and arginine biosynthesis are significantly affected in HTG patients (Table 2). All these events are directly or indirectly associated with increased oxidative stress and inflammation. It was confirmed by increased levels of PGF-2α and leukotriene B_4 in HTG patients. In contrast, TCE supplementation

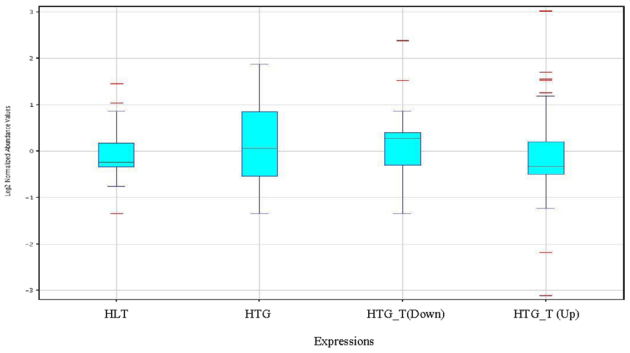

Fig. 5 Box-whisker plot also showed that HTG_T_UP proteins had highest intergroup variation as evidenced by extended whiskers across lower and upper quartiles

significantly modulated the PGF-2α, leukotriene B_4, BCAA, arginine, and hypotaurine levels ($p < 0.05$) in HTG patients (Table S2). Leukotriene B_4 is reported to increase oxidative stress through the downregulation of thiamine [17] and up-regulation of ether lipids, lysophosphatidylethanolamines (LysoPE), and diacylglycerols (DG) as observed in the current study (Table 2). LysoPE and DG are reported to responsible for abnormal metabolic regulation and obesity [27]. Increased lipid peroxidation was further supported by increased levels of MDA, capryloylglycine and aminoadipic acid, the markers of disorders in mitochondrial fatty acid β-oxidation and insulin resistance (Table 2). High levels of lipid peroxides in HTG patients also induce ferroptosis, a less explored apoptosis phenomenon [28]. A previous study also showed that oxidative stress is a primary event in the HTG patients confirmed by [26].

Fatty acid metabolism is primarily regulated by PPARs present in peroxisomes [29]. PPARs also regulate lipolysis and bile acid secretion and synthesis [30]. In HTG patients all three events i.e. peroxisome biogenesis, lipolysis in adipocytes, and bile acid secretion and synthesis was found to be disturbed (Table S4). Moreover, metabolomics profiles indicated the disturbed function of ATP-binding cassette transporter (ABC) in HTG patients (Table S4). It was the well-known fact that increased TGs and reduced HDL levels are related to mutation or depressed ABC function, particularly ABCA1, membrane integral protein required for nascent HDL apolipoprotein A-I particle formation [31]. Depressed ABCA1 is reported to increase lipid rafts in the plasma membrane and provide access to inflammatory signals to increase inflammation [28, 29]. TCE intervention downregulated the levels of peroxisomal N-acetyl-spermine/spermidine and increased the levels of ApoA1 in HTG individuals and downregulate the FGF2 in HTG_T individuals (Table 6; Fig. 6).

In previous studies, it was observed that HTG reduces the retaining power of vitamins that increased their excretion in urine. Previous studies reported that a low level of vitamin B6 is linked to the increased risk of coronary artery disease (CAD) [32]. Decreased vitamin B6 levels are directly linked to the decreased response of the renin-angiotensin system [33]. The renin-angiotensin-aldosterone system (RAAS) plays an important role to regulate several pathophysiologic changes related to the progression of renal disease, blood volume, and systemic vascular resistance [33]. High calcium concentrations have been reported to inhibit renin release and stimulate aldosterone release [34]. Hence, these are events interrelated with the cGMP-PKG signaling pathway found to be affected in HTG patients (Table S4). Increased cGMP phosphorylates the protein substrate responsible for the cellular damages and abnormal calcium regulation [35]. Defective RAAS and cGMP-PKG signaling are also associated with the increased interstitial fibrosis, thickening of coronary arteries contribute towards the hypertrophic cardiomyopathy (HCM) [36, 37].

As observed in metabolomics studies, proteome profile also indicated the compromised peroxisome biogenesis in HTG patients. Peroxisomes specific protein MPV17-like protein and bifunctional epoxide hydrolase 2 and Polyamine oxidase splice variant 11 were found to be down-regulated in HTG_T patients (Table 6). However, TCE supplementation increased the levels of all three proteins important in trafficking proteins to the peroxisome and to maintain arachidonic acid signaling via binding with PAX2 and ADAM10. Also, ADAM10 controls the expression of MMP3, hence responsible for the regulation of cholesterol metabolism and ECM remodeling. Similarly, polyamine catabolism has been reported to improve the PGC-1α activity and decrease triglycerides level and normalize the bile acid metabolism [38, 39]. Hence, debilitated peroxisome function increased the TG levels that lead to oxidative stress and insulin resistance in HTG patients.

Insulin resistance impaired the PI3K dependent Akt phosphorylation [40]. Proteomics analysis showed the downregulation of insulin receptors in HTG patients (Table S4). It was further confirmed by the up-regulated expression of E3 ligases under transcription control of FoxO3, a downstream target of Akt [41]. Reduced Akt signaling resulted in the increase of RNA binding motif protein 25 in HTG to promote the upregulation of BCL-2 and suppress the C-terminal-binding protein 2 in HTG individuals essential for the PPAR signaling and differentiation of adipocytes [42]. Moreover, reduced INSR expression decline the expression of SKIL protein associated with LATS2 responsible for the Wnt and protein kinase signaling. Also, reduced expression of NUPR were found in HTG individual. Besides NUPR control the expression of MMP13 contributes towards the ECM remodeling (Fig. 6). Similarly, decreased FBL in HTG_T downregulate the expression of TP53, leads to increase expression of NUMB in HTG_T and reduces the

Table 2 Differentially expressed metabolites in various groups without missing values after PLS-DA and Bonferroni multiple testing according to their significance and variability. All metabolites are identified using various databases in ESI + mode ($p < 0.05$)

Sr. No	Tentative Compounds	Mass	RT	KEGG ID	p (Corr)	Fold Change		
						HTG vs HLT	HTG_T vs HLT	HTG_T vs HTG
1	Hypotaurine	109.0019	5.01	C00519	2.40E-18	1.39	9.31	6.69
2	L-Valine	117.0795	5.54	C00183	2.40E-18	1.3	−9.16	−6.99
3	L-Cysteine	121.0907	38.2	C00097	3.24E-05	−2.07	−1.32	−1.56
4	Nicotinic acid	123.0796	38.0	C00253	6.87E-05	1.13	2.82	2.5
5	Acetylphosphate	139.9101	5.02	C00227	7.13E-15	−1.44	7.36	5.08
6	Mevalonic acid	148.0162	35.4	C00418	6.97E-12	2.1	3.3	−1.56
7	L-Carnitine	161.105	5.57	–	7.90E-16	1.39	7.09	5.10
8	3-Hydroxysuberic acid	190.0697	5.25	–	3.69E-14	−1.49	−7.32	−4.89
9	5-Dodecenoic acid	197.9326	5.01	C02679	1.52E-18	1.31	9.19	6.97
10	Capryloylglycine	201.1733	38.1	–	6.85E-06	2.35	1.45	1.61
11	Sebacic acid	202.0452	5.41	C08277	1.52E-18	−1.32	9.19	6.94
12	L-Acetylcarnitine	203.1164	7.83	C02571	1.89E-18	−1.2	−4.96	−6
13	2-Oxo-3-hydroxy-4- phosphobutanoic acid	213.9108	5.02	C06054	1.52E-18	1.29	9.12	7.06
14	12-Hydroxy dodecanoic acid	216.0994	35.8	C08317	1.31E-05	−1.02	2.97	3.05
15	2,5-Dichloro-4-oxohex-2-enedioate	225.9448	37.9	C12835	5.83E-04	1.71	1.41	−2.42
16	Deoxyuridine	227.9262	5.01	C00526	1.89E-18	1.36	9.25	−6.79
17	5-Hydroxyindoleacetyl glycine	248.1016	5.75	C05832	1.33E-17	−1.13	6.92	6.07
18	Deoxyinosine	252.2487	33.9	C05512	2.77E-11	1.01	3.96	3.89
19	Vaccenic acid	281.9015	5.16	C08367	1.03E-11	−1.47	−3.43	2.33
20	Unknown	287.9149	5.14	–	1.18E-17	−1.09	5.21	5.70
21	N-Acetyl neuraminic acid	309.197	19.6	C19910	4.93E-09	−1.46	5.79	8.46
22	Unknown	333.9084	5.11	–	1.18E-17	−1.09	5.21	5.70
23	Prostaglandin A1	336.2671	27.0	C04685	1.98E-09	1.48	5.67	8.44
24	Unknown	343.8683	5.02	–	1.89E-18	−1.17	4.78	5.61
25	Tricosanoic acid	354.0638	32.8	–	2.49E-04	2.95	−3.25	−1.1
26	Cortisone	360.2712	27.0	C00762	6.16E-09	−1.52	5.5	8.4
27	Nervonic acid	366.3537	34.0	C08323	2.00E-10	−1.53	5.49	8.4
28	Ferulic acid 4-O-glucuronide	370.0947	34.4	–	1.37E-04	−3.73	−3.23	−1.15
29	16-phenoxy tetranor Prostaglandin A2	370.0979	34.4	–	3.00E-04	−2.97	−3.23	1.08
30	5α-Cholestanol	388.3389	31.3	–	5.45E-05	−1.67	1.82	3.04
31	Nutriacholic acid	390.2816	35.4	–	0.011724	2.52	2.67	1.06
32	Ursodeoxycholic acid	393.2926	27.1	C07880	8.76E-06	1.48	5.65	8.42
33	1-[3-(3,7-dimethylocta-2,6-dien-1-yl)-2,4,6-trihydroxyphenyl]-3-phenylpropan-1-one	394.2349	28.5	–	1.89E-18	1.56	9.53	6.08
34	LPA(P-16:0e/0:0)	394.2381	34.1	–	1.89E-18	−1.56	−9.53	−6.08
35	3a,7a-Dihydroxy-5b-cholestane	404.3697	33.9	–	2.42E-11	−2.20	−3.30	−1.49
36	Unknown	412.2588	33.9	–	4.70E-04	−3.67	−3.58	1.02
37	LysoPC(10:0)	412.2598	33.9	–	4.70E-04	3.67	3.58	−1.02
38	Folic acid	441.3099	31.5	C00504	1.25E-11	−2.31	−3.35	1.44
39	Unknowm	441.871	5.0	–	1.89E-18	1.34	9.23	6.88
40	3a,7a,12a-Trihydroxy-5b-cholestanoic acid	450.3721	34.0	C04722	9.28E-12	1.59	3.49	2.19
41	10,11-Dihydro-12R-hydroxy-leukotriene E4	457.3778	31.1	–	5.66E-16	−1.48	−5.67	8.44
42	6-Dehydrotestosterone glucuronide	462.333	34.1	C03033	9.28E-12	−1.09	4.23	4.64
43	α-Tocopherol acetate	472.3564	29.7	C13202	4.61E-18	2.47	2.08	5.15
44	LysoPE(0:0/18:2(9Z,12Z)	477.2865	27.1	–	1.28E-04	1.41	5.95	−8.43
45	11-Oxo-androsterone glucuronide	480.3862	4.9	–	8.37E-06	−2.39	−1.47	1.62
46	PA(20:4(5Z,8Z,11Z,14Z)e/2:0)	486.3378	32.7	–	3.30E-04	3.78	3.79	1
47	Citicoline	488.3536	34.1	C00307	3.99E-04	3.71	3.75	1

Table 2 (continued)

Sr. No	Tentative Compounds	Mass	RT	KEGG ID	*p* (Corr)	Fold Change		
						HTG vs HLT	HTG_T vs HLT	HTG_T vs HTG
48	LysoPE(0:0/20:4(8Z,11Z,14Z,17Z))	501.2867	27.1	–	2.40E-18	1.23	−8.95	−7.26
49	LysoPE(20:4(8Z,11Z,14Z,17Z)/0:0)	501.3675	27.1	–	8.50E-05	1.43	5.86	8.43
50	Unknown	502.4023	33.9	–	1.87E-09	−4.22	−4.20	1.01
51	Unknown	514.3646	34.1	–	3.99E-04	−3.77	−3.17	1.01
52	LysoPE(0:0/22:6(4Z,7Z,10Z,13Z,16Z,19Z))	525.2868	26.9	–	3.47E-04	1.49	5.54	8.31
53	LysoPE(0:0/22:4(7Z,10Z,13Z,16Z))	529.34	30.7	–	2.97E-18	1.45	3.83	−5.59
54	unknown	534.3972	33.9	–	4.30E-12	−2.86	−3.88	−1.35
55	Unknown	545.3973	30.1	–	7.72E-13	1.22	−5.07	6.23
56	LysoPC(22:4(7Z,10Z,13Z,16Z))	571.8308	5.02	C04230	1.89E-18	−1.34	−9.22	−6.85
57	Bilirubin	584.265	35.8	C00486	0.048275	2.36	2.42	−1.02
58	Unidentified	587.8134	5.02	–	1.89E-18	1.33	−9.19	−6.9
59	DG(20:4(5Z,8Z,11Z,14Z)/15:0/0:0)	602.291	25.6	–	6.85E-06	1.47	5.7	8.43
60	Unknown	603.3998	29.6	–	2.97E-18	1.31	9.16	6.97
61	DG(18:2n6/0:0/22:6n3)	678.5129	36.5	–	0.003148	2.14	2.89	−1.34
62	PE(18:3(9Z,12Z,15Z)/14:0)	685.8087	5.1	C00350	5.32E-18	1.091	−5.16	−5.64
63	PC(14:0/15:0)	691.4524	29.5	C00157	2.16E-18	−1.31	−9.17	−6.96
64	CerP(d18:1/22:0)	701.7883	5.02	–	2.97E-18	1.09	−6.82	−6.21
65	PE(18:4(6Z,9Z,12Z,15Z)/P-18:1(9Z))	721.4979	29.7	C00350	1.89E-18	−1.27	9.07	7.11
66	PE(DiMe(11,3)/DiMe(9,3)	795.5195	38.5	–	1.08E-05	−1.49	5.64	8.42
67	PE(20:5(5Z,8Z,11Z,14Z,17Z)/24:1(15Z))	847.5421	37.9	C00350	1.03E-11	−1.43	5.91	8.48
68	Nicotinamide ribotide	336.2671	27.1	C00455	1.18E-17	1.09	−5.21	−5.7
69	Aminoadipic acid	117.0795	5.5	C00956	7.90E-16	1.39	−7.09	−5.1

Note: LysoPC(10:0): 1-decanoyl-sn-glycero-3-phosphocholine; LysoPE(0:0/18:2(9Z,12Z): 2-linoleoyl-sn-glycero-3-phosphoethanolamine; PA(20:4(5Z,8Z,11Z,14Z)e/2:0): 2-Acetyl-1-(5Z,8Z,11Z,14Z-eicosatetraenyl)-sn-glycero-phosphate; DG: Diacylglycerol; PE(18:3(9Z,12Z,15Z)/14:0): phophatidylethanolamine (18:3(9Z,12Z,15Z)/14:0); CerP(d18:1/22:0): ceramide phosphate (N-docosanoylsphingosine-1-phosphate)

Table 3 Table with quantity of each of IsoPs analysed under study categories in variety of samples in both ion polarity modes expressed in µg/mL with mean ± SD ($p < 0.01$). 8-iPGA1: 8-iso Prostaglandin A1; PGF2α: Prostaglandin $F_2\alpha$; $PGF_{2\alpha}$-IV: Prostaglandin F2α-IV; $PGF_1\alpha$: Prostaglandin F1α; PGB1: Prostaglandin B1

S. No.	Name of IsoPs	Plasma +ve mode			Plasma -ve mode			*p* value
		HLT	HTG	HTG_T	HLT	HTG	HTG _T	
1.	8-iso PGA_1	–	–	–	–	–	–	–
2.	$PGF_2\alpha$				0.33 ± 0.018	0.45 ± 0.014	0.37 ± 0.011	< 0.0001
3.	8,12-iso$PGF_2\alpha$-VI	5.319 ± 1.718	6.078 ± 3.434	3.607 ± 0.210	–	–	–	< 0.0001
4.	8-epi $PGF_{1\alpha}$	4.446 ± 1.58	5.935 ± 1.41	2.237 ± 1.41	–	–	–	< 0.0001
5.	PGB1				0.654 ± 6.33	1.344 ± 0.40	5.687 ± 1.41	< 0.0001

EHD2 expression, hence increase the GLUT 4 sensitivity (Fig. 6).

PI3K is a downstream target of INSR, hence increased expression of INSR also activates PI3K [43]. Catalytic subunit p110δ of PI3K is the activator of Rap GTPase, important in the cytoskeletal arrangement [44]. INSR as well as RAP guanine nucleotide exchange factor 2 (Repac) another activator of Rap1 signaling were found to be down-regulated in HTG patients (Table 5). However, TCE intervention activated PI3K being the downstream target of INSR, and increased the expression levels of Repgef2, to activate the Rap1 signaling pathway. Furthermore, decreased levels of 1-phosphatidylinositol 4,5-bisphosphate phosphodiesterase beta-3 (PLC) in HTG patients confirmed the depressed signaling of Rap1 (Table 5). The present study showed that TCE treatment could not

Table 4 Table is showing the quantity of each metabolites analysed in both ion polarity modes and expressed in µg/mL with Mean ± SD form ($p < 0.01$)

S. No.	Metabolites	KEGG ID	HTL	HTG	HTG_T	Reference value (µg/mL)
1.	β-Alanine	C00099	25.08 ± 1.68	31.67 ± 1.87	24.189 ± 1.5	45.90
2.	L-Serine	C00065	22.03 ± 1.61	10.18 ± 1.27	15.44 ± 1.85	15.91
3.	L-Proline	C00148	53.21 ± 2.77	61.80 ± 0.96	54.81 ± 2.17	41.40
4.	L-Valine	C00183	23.28 ± 1.59	31.97 ± 1.97	24.72 ± 1.46	41.02
5.	L-Threonine	C00188	15.81 ± 1.36	18.66 ± 1.53	36.34 ± 1.38	28.58
6.	Taurine	C00245	41.84 ± 3.63	38.03 ± 2.73	26.09 ± 0.72	16.26
7.	L-Leucine	C00123	35.98 ± 2.49	53.65 ± 2.57	44.49 ± 3.68	22.30
8.	L-Ornithine	C00077	17.88 ± 1.85	43.59 ± 2.08	34.30 ± 2.26	11.89
9.	L-Aspartic acid	C00049	13.98 ± 0.92	19.03 ± 2.63	15.76 ± 2.023	3.46
10.	L-Lysine	C00047	12.43 ± 1.03	17.27 ± 0.94	24.55 ± 1.93	42.39
11.	L-Glutamic acid	C00025	5.03 ± 0.39	7.61 ± 0.58	9.79 ± 0.65	20.59
12.	L-Methionine	C00073	5.82 ± 1.09	5.39 ± 0.45	2.75 ± 0.37	4.4
13.	L-Histidine	C00135	30.95 ± 1.87	39.71 ± 0.29	44.69 ± 0.45	18.6
14.	L-Phenylalanine	C00079	12.95 ± 0.99	12.58 ± 1.05	7.72 ± 0.81	14.20
15.	L-Arginine	C00062	20.08 ± 1.93	12.96 ± 1.19	23.03 ± 1.79	21.00
16.	L-Tyrosine	C00082	20.75 ± 1.87	16.28 ± 0.93	–	20.00
17.	L-Tryptophan	C00078	13.64 ± 1.44	17.85 ± 1.03	4.09 ± 1.21	22.40
18.	L-Cystine	C00491	3.46 ± 1.5	3.49 ± 0.35	5.45 ± 0.32	15.60
19.	L-Pyroglutamic acid	C01879	3.05 ± 0.98	10.07 ± 2.32	6.09 ± 0.6	11.20
20.	Nicotinamide (ng/mL)	C00153	40.26 ± 1.134	32.01 ± 1.24	38.47 ± 0.67	53.00 (ng/mL)
21.	DL-5-HydroxyLysine	C16741	0.39 ± 0.09	0.46 ± 0.08	0.46 ± 0.06	0.405
22.	L-Homocysteic acid	C16511	1.25 ± 0.90	2.12 ± 0.73	0.93 ± 0.63	4.00
23.	L-Glutathione oxidized	C00127	6.58 ± 0.14	5.34 ± 0.17	5.54 ± 0.45	1.22
24.	L-Glutathione reduced	–	2.67 ± 0.28	2.06 ± 0.46	2.16 ± 0.55	1.22
25.	Hexanal (ng/mL)	C02373	36.94 ± 2.28	40.95 ± 1.87	23.76 ± 1.51	52 (ng/mL)
26.	Testosterone	C00535	3.76 ± 0.80	2.73 ± 0.98	2.89 ± 0.77	2.60
27.	Malondialdehyde (ng/mL)	C19440	397.1 ± 6.51	460.65 ± 6.23	356.49 ± 10.8	389 (ng/mL)
28.	L-Citrulline	C00327	10.21 ± 0.20	11.65 ± 0.44	9.28 ± 0.59	12.20
29	Linoleic acid	C01595	60.84 ± 4.91	58.77 ± 6.45	10.56 ± 0.92	58.0
		-ve	71.92 ± 10.82	55.54 ± 5.32	51.83 ± 4.09	
30.	Carnitine	C00318	4.56 ± 0.71	9.87 ± 1.84	3.06 ± 0.28	7.25
31	DL-Homocysteine	C05330	9.55 ± 1.09	7.09 ± 6.93	–	1.40
		-ve	2.97 ± 0.44	1.29 ± 1.33	0.67 ± 0.95	–
32.	8-Hydroxy-2-deoxyguanosine	–	1.43 ± 0.64	1.64 ± 0.73	0.97 ± 0.32	0.84 (ng/mL)
33.	Cysteineglycine	C01419	14.66 ± 0.90	19.01 ± 1.16	16.93 ± 1.26	12.40
34.	Porphobilinogen	C00931	0.95 ± 0.38	0.92 ± 0.39	1.50 ± 0.65	0.700
35.	Bilirubin	C00486	10.53 ± 1.96	17.27 ± 1.92	0	8.70
		-ve	8.93 ± 0.79	14.93 ± 1.36	10.91 ± 0.80	–
36.	Protoporphyrin IX	C02191	0.31 ± 0.05	0.23 ± 0.06	0.35 ± 0.07	0.61
37.	β-Carotene	C02094	0.52 ± 0.19	0.35 ± 0.09	0.52 ± 0.08	0.63
38.	α -tocopherol	C02477	16.66 ± 2.81	12.64 ± 1.66	0	21.10
39.	γ- tocopherol	C02483	5.87 ± 0.76	3.45 ± 0.73	5.44 ± 2.57	3.00
40.	Cholesterol	C00187	1838.9 ± 92.4	2109.3 ± 76.9	1855.3 ± 63.6	4446.0
41.	Lipoic acid	C16241	6.37 ± 2.23	4.55 ± 1.28	4.8 ± 1.66	NR
42.	Glycocholate	C01921	0.36 ± 0.13	0.35 ± 0.14	0.24 ± 0.09	0.40
43.	Glycitin	–	5.35 ± 0.45	4.67 ± 0.33	0	NR
44.	Arachidonic acid	C00219	12.8 ± 0.29	13.57 ± 0.49	0	12.1
		-ve	7.19 ± 0.48	8.02 ± 0.47	2.93 ± 0.67	
45.	Leukotriene B_4 (pg/mL)	C02165 -ve	99.44 ± 4.7	139.59 ± 8.05	110.10 ± 5.7	67.3 (pg/mL)

Table 5 The differentially expressed proteins in HTG group in comparison to healthy (HTL) group

S No	MS/MS Score	SPI (%)	Spectrum Intensity	% AA coverage	MW (Da)	Protein Name	Uniprot ID	FC in HT
1.	30.53	88.7	4.99e+004	3	107,905.0	ALS2CL	Q60I27	−4.0
2.	102.61	90.4	4.62e+004	27	30,778.0	APOA1	P02647	−4.0
3.	22.16	90.6	2.95e+004	13	16,508.1	ARP-PCAR	Q9UMX4	−1.8
4.	19.34	94.1	4.89e+005	3	58,024.5	CCT6A	P40227	−2.8
5.	27.27	77.0	3.13e+004	11	316,416.8	CENPE	Q02224	−6.3
6.	19.15	79.3	1.65e+004	3	207,433.7	CHD1	O14646	1.9
7.	29.22	93.2	4.73e+004	12	226,037.5	CKAP5	Q14008	−4.0
8.	33.79	85.0	1.90e+005	2	161,790.5	COL4A5	P29400	2.0
9.	34.59	88.1	1.72e+005	2	106,187.3	CTBP2	P56545	−4.0
10.	26.40	69.9	1.99e+004	4	532,841.8	DYNC1H1	Q14204	−4.0
11.	18.59	94.1	4.64e+004	5	33,818.4	FBL	P22087	2.8
12.	29.84	68.0	3.77e+004	2	532,231.0	HERC1	Q15751	2.2
13.	19.50	90.9	4.86e+005	0	546,378.1	HMCN2	Q8NDA2	4.0
14.	18.08	83.8	1.01e+005	12	159,709.7	INSR	P06213	−2.1
15.	18.51	94.4	1.28e+005	11	36,869.9	JMJD8	Q96S16	−2.4
16.	18.47	92.0	4.80e+004	13	17,572.5	LMBRD2	Q68DH5	−1.8
17.	18.32	83.7	4.64e+004	3	110,136.6	MIB1	Q86YT6	1.9
18.	18.91	78.7	1.21e+004	5	47,995.1	MTX1	Q13505	−1.9
19.	29.28	99.3	2.44e+006	8	49,433.2	NADK2	Q4G0N4	4.0
20.	44.92	86.9	2.94e+005	12	264,800.3	NBAS	A2RRP1	−4.0
21.	20.19	90.1	5.95e+004	13	16,395.7	NPPA	A0A0P6J1W3	−1.9
22.	26.54	84.0	2.52e+004	20	8872.8	NUPR1	O60356	−1.9
23.	37.51	99.8	9.99e+005	5	129,468.6	CO1A2	P08123	−4.0
24.	19.47	92.4	3.01e+004	16	12,202.9	PAOX	Q6QHF9	−4.0
25.	19.47	92.4	3.01e+004	2	70,290.2	PAOX	Q6QHF9	3.7
26.	20.45	77.2	3.05e+004	2	136,065.1	PCDH9	Q9HC56	−2.5
27.	27.29	89.1	5.26e+004	15	61,223.7	PDE9A	O76083	−1.8
28.	20.26	72.9	2.29e+005	3	138,799.7	PLCB3	Q01970	−5.5
29.	21.24	87.5	2.85e+004	8	68,464.1	PPM2C	Q6P1N1	−1.9
30.	33.44	91.9	7.29e+004	2	227,842.7	PRRC2A	P48634	−4.0
31.	66.19	91.1	2.34e+004	5	190,718.9	RAPGEF2	Q9Y4G8	−4.0
32.	26.70	86.7	3.98e+004	2	114,803.8	RBM25	P49756	15.1
33.	57.49	90.3	4.27e+005	2	187,671.9	RIMS2	Q9UQ26	4.0
34.	19.65	88.3	1.72e+004	10	24,678.6	SLC25A43	Q8WUT9	−4.0
35.	33.88	91.1	2.95e+005	12	42,896.4	SKIL	P12757	−1.9
36.	18.91	93.6	1.59e+004	7	43,366.0	SOHLH1	Q5JUK2	1.7
37.	19.67	82.0	1.61e+004	16	22,195.9	SYNGR1	O43759	−4.0
38.	35.19	94.6	3.37e+005	3	218,220.6	TCF20	Q9UGU0	4.0

normalize the levels of PLC but increased its levels to 2 fold as compared to HTG patients, hence contributed to the activation of the Rap1 signaling pathway.

It has been reported that Rap1 is essential for Extracellular matrix (ECM) molding including cell adhesion and cell junctions [45]. Hence, disrupted Rap1 signaling led to down-regulation of ECM specific α-1 type 2 collagen, transthyretin,pre-pro-α-2 type I collagen, protocadherin-9, CENPE, CKAP5, and DYNC1H1 in HTG individual (Table 5) and led to ECM hardening. Moreover, the present study indicated that TCE restored the expression levels of collagen α-3(V) chain, T-complex protein 1, transmembrane protease serine 13, transmembrane protein 16H, etc. (Table 6, Fig. 6). TCE supplementation increases the expression of TTN through MYL1 to regulate skeletal muscle differentiation. Also, downregulated NTN3 and PODN in HTG_T individuals lead to

Table 6 The differentially expressed proteins in HTG_T group in comparison to HTG group

S No	MS/MS Score	SPI (%)	Spectrum Intensity	% AA coverage	Protein MW (Da)	Gene Name	Uniprot ID	FC in HTT
1.	17.15	96.7	4.04e+004	3	65,628.8	ANO8	Q9HCE9	3.9
2.	101.27	90.2	3.08e+004	31	30,778.0	APOA1	P02647	1.9
3.	22.16	90.6	2.95e+004	13	16,508.1	Apoptotic-related protein PCAR	Q9UMX4	−4.0
4.	18.43	97.8	1.14e+004	8	17,369.1	ATPSCKMT	Q6P4H8	4.0
5.	11.17	70.3	8.40e+003	5	56,748.0	BTNL8	Q6UX41	4.1
6.	16.86	80.7	1.60e+004	5	35,880.7	C1QBP	Q07021	4.0
7.	18.56	91.5	1.01e+005	3	57,793.7	CCT6B	Q92526	4.2
8.	24.87	93.1	1.53e+004	4	37,237.1	CEACAM6	P40199	−3.8
9.	27.27	77.0	3.13e+004	1	316,416.8	CENPE	Q02224	−4.1
10.	19.15	79.3	1.65e+004	1	207,433.7	CHD1	O14646	−4.2
11.	29.22	93.2	4.73e+004	1	226,037.5	CKAP5	Q14008	4.0
12.	19.74	95.9	2.10e+004	4	64,479.3	COL2A1	P02458	−3.9
13.	31.91	74.8	2.15e+005	2	172,121.6	COL5A3	P25940	4.0
14.	17.57	91.1	8.18e+004	6	15,349.6	CSDA1/YBX3	A0A024RAQ1	4.2
15.	17.51	78.4	4.05e+004	2	90,174.4	DACT1	Q9NYF0	4.0
16.	18.71	80.8	4.39e+004	1	89,251.1	DDX21	Q9NR30	4.3
17.	17.63	80.0	7.79e+004	1	106,866.0	DENND2C	Q68D51	1.9
18.	33.35	95.3	1.04e+005	9	40,339.9	EDG-7	Q9NRB8	4.0
19.	20.07	79.7	1.44e+004	4	61,161.7	EHD2	Q9NZN4	−3.9
20.	19.59	93.2	2.53e+004	1	99,491.5	EPB41L4B	Q9H709	4.1
21.	19.98	92.6	3.55e+004	3	56,987.6	EPHX2	P34913	4.1
23.	18.59	94.1	4.64e+004	5	33,818.4	FBL	P22087	−3.8
24	18.09	90.4	3.22e+004	19	17,412.1	FGF2	P09038	−4.0
25	10.17	95.1	5.87e+003	1	124,762.3	FHDC1	Q9C0D6	3.8
26.	19.80	81.7	3.54e+004	4	69,422.7	FLJ00357	Q6ZMJ9	4.0
27.	17.23	87.5	2.33e+004	6	28,490.7	GALNT10	Q4G0E1	4.4
28	19.67	88.6	2.36e+004	1	111,998.6	GLB1L3	Q8NCI6	3.9
29.	17.17	84.4	1.72e+004	4	39,065.2	*GPR57*	Q9P1P4	−4.2
30.	19.56	77.3	4.29e+004	2	103,109.6	GRIA2	P42262	−4.5
31.	18.26	76.4	6.39e+004	32	5497.3	hCG1745092	P30050	3.9
32.	12.49	93.5	2.89e+004	8	33,408.3	hCG2044603	Q8NH61	3.6
33.	29.84	68.0	3.77e+004	0	532,231.0	HERC1	Q15751	−4.0
34.	18.51	83.9	1.81e+004	9	35,844.9	HMG20B	Q9P0W2	−4.3
35.	12.93	78.4	3.56e+003	7	12,905.7	IGHV4–4	A0A075B6R2	4.1
36.	19.35	79.2	2.79e+004	4	36,869.9	JMJD8	Q96S16	4.0
37.	18.47	92.0	4.80e+004	13.0	17,572.5	LMBRD2	Q68DH5	−4.0
38.	16.9	82.6	1.46e+005	3	68,023.7	MEN1	O00255	5.1
39.	18.32	83.7	4.64e+004	2	110,136.6	MIB1	Q86YT6	−4.0
40.	16.45	89.4	4.26e+004	8	22,115.8	MPV17L	Q2QL34	4.0
41.	18.91	78.7	1.21e+004	5	47,995.1	MTX1	Q13505	−3.9
42.	16.05	70.4	5.57e+004	1	149,367.9	MYBBP1A	Q9BQG0	4.1
43.	17.46	84.1	4.32e+004	0	200,332.6	NALCN	Q8IZF0	4.2
44.	20.19	90.1	5.95e+004	13	16,395.7	NPPA	A0A0P6J1W3	−3.9
45.	20.16	84.5	1.75e+004	5	61,466.5	NTN3	O00634	−4.2
46.	19.24	86.0	5.86e+004	2	70,804.2	NUMB	P49757	4.4
47.	26.54	84.0	2.52e+004	20	8872.8	NUPR1	O60356	−4.3
48.	19.47	92.4	3.01e+004	2	70,290.2	PAOX	Q6QHF9	−3.5
49.	20.45	77.2	3.05e+004	2	136,065.1	PCDH9	Q9HC56	−4.0

Table 6 (continued)

S No	MS/MS Score	SPI (%)	Spectrum Intensity	% AA coverage	Protein MW (Da)	Gene Name	Uniprot ID	FC in HTT
50.	27.29	89.1	5.26e+004	5	61,223.7	PDE9A	O76083	−4.2
51.	19.36	93.4	1.73e+004	4	31,700.4	PITPNB	P48739	4.3
52.	20.26	72.9	2.29e+005	1	138,799.7	PLCB3	Q01970	−3.6
53.	17.19	78.7	2.73e+004	1	146,897.2	PLEKHA5	Q9HAU0	4.0
54.	39.04	91.4	1.40e+005	11	40,671.9	PODN	Q7Z5L7	−4.0
55.	19.04	89.7	5.67e+004	4	41,970.3	POLB	P06746	−3.5
56.	17.30	85.0	1.43e+004	9	15,131.1	POLR2M	P0CAP2	3.6
57.	16.91	85.4	1.93e+004	7	22,949.1	PSMB3	P49720	4.0
58.	20.39	85.7	1.49e+004	17	16,022.6	PXT1	Q8NFP0	−4.1
59.	57.49	90.3	4.27e+005	2	187,671.9	RIMS2	Q9UQ26	−4.0
60.	16.01	79.5	2.05e+004	4	46,629.0	RNF149	Q8NC42	4.0
61.	17.19	81.1	3.51e+004	4	29,245.7	RNF187	Q5TA31	4.2
62.	20.65	94.9	6.47e+004	11	9357.8	RPL19	J3KTE4	−3.8
63.	21.72	97.5	6.20e+005	1	50,246.5	SBK1	Q52WX2	4.1
64.	17.82	91.6	9.22e+005	4	42,896.4	SNO1/SKIL	P12757	3.8
65.	18.91	93.6	1.59e+004	7	43,366.0	SOLH	O75808	−4.3
66.	7.38	90.0	1.25e+004	1	16,844.4	SSPOP	A2VEC9	4.3
67.	18.30	94.2	4.52e+004	2	63,153.5	TMPRSS13	Q9BYE2	3.4
68.	31.60	84.8	3.56e+005	1	228,584.9	TRIP12	Q14669	4.0
69.	34.73	93.1	1.11e+006	1	3,994,674.4	TTN	Q8WZ42	4.0
70.	36.16	84.4	3.12e+004	26.0	14,957.0	TTR	P02766	−1.9
71.	18.34	89.1	8.99e+004	1	77,154.6	TWNK	Q96RR1	4.1
72.	17.13	74.7	4.45e+004	1	119,171.4	ZBTB21	Q9ULJ3	4.0
73.	24.78	93.1	3.54e+004	6	54,714.9	ZNF517	Q6ZMY9	−4.0

reduction in expression of RBM25 as well BCL2L1, to eliminate the prevalence of apoptosis. Moreover, the present study also found that TCE supplementation increases the expression of MYBBP1A, to regulate the intrinsic pathway of apoptosis through p53 signaling. In association with MYBBP1A, DDX21 promote the expression of KLK2/3 to stimulate the androgen receptor (AR). Activated AR upregulates the DCNT2 expression also supported by MEN1 in HTG_T individuals to control the ECM remodeling (Fig. 6).

It has been found that alkaloidal constituents, (−)-epicatechin, secoisolariciresinol, and an arabinogalactan polysaccharide from *T. cordifolia* were reported to reduce oxidative stress and lipid peroxidation [12]. Surprisingly, the overall analysis also illustrated the positive effects of TCE on the hypoxia-inducible factor 1 (HIF-1) signaling pathway. Hence, HTG impaired HIF-1 activation or vice-versa like T2DM that may lead to cardiomyopathy in the individuals [46]. Similarly, TCE administration also decreases the TTR protein responsible for the upregulation of IL-6 in HTG_T individuals (Fig. 6).

Genetic Association Database (GAD) analysis of proteome data showed the down-regulated proteins in HTG groups are associated with hyperlipidemia, obesity, brain aneurysm, kidney failure, chronic, diabetes type 2 (T2DM), cardiovascular diseases due to disturbed regulation of APOA1 and INSR. However, ApoA1 was also reported to activate FoxO1 which increases insulin secretion and β-cell regeneration [47].

Combine analysis of proteomics and metabolomics data using Metascape plugin in Cytoscape and Metaboanalyst (online software) illustrated that high TG levels disturbed the PI3K-Akt signaling pathway independent of cholesterol levels (Table S5). Disrupted PI3K-Akt signaling in HTG patients affected glucose, lipid, and protein metabolism along with cell proliferation and survival. It leads to oxidative stress, inflammation, and insulin resistance which induce T2DM and lead to activation of the AGE-RAGE signaling pathway (Table S5). The present study found that TC supplementation increased the expression of ApoA1 which regulate the expression of INSR through the NR1H4 gene. Moreover, protein catabolism was found to be increased due to the activation of FoxO3, downstream target of Akt, evident by increased levels of E3 ligases. ApoA1 was also reported to activate FoxO1 which increases insulin secretion and β-cell regeneration [48]. Also, protoberberine alkaloid of TCE seems to act similarly to

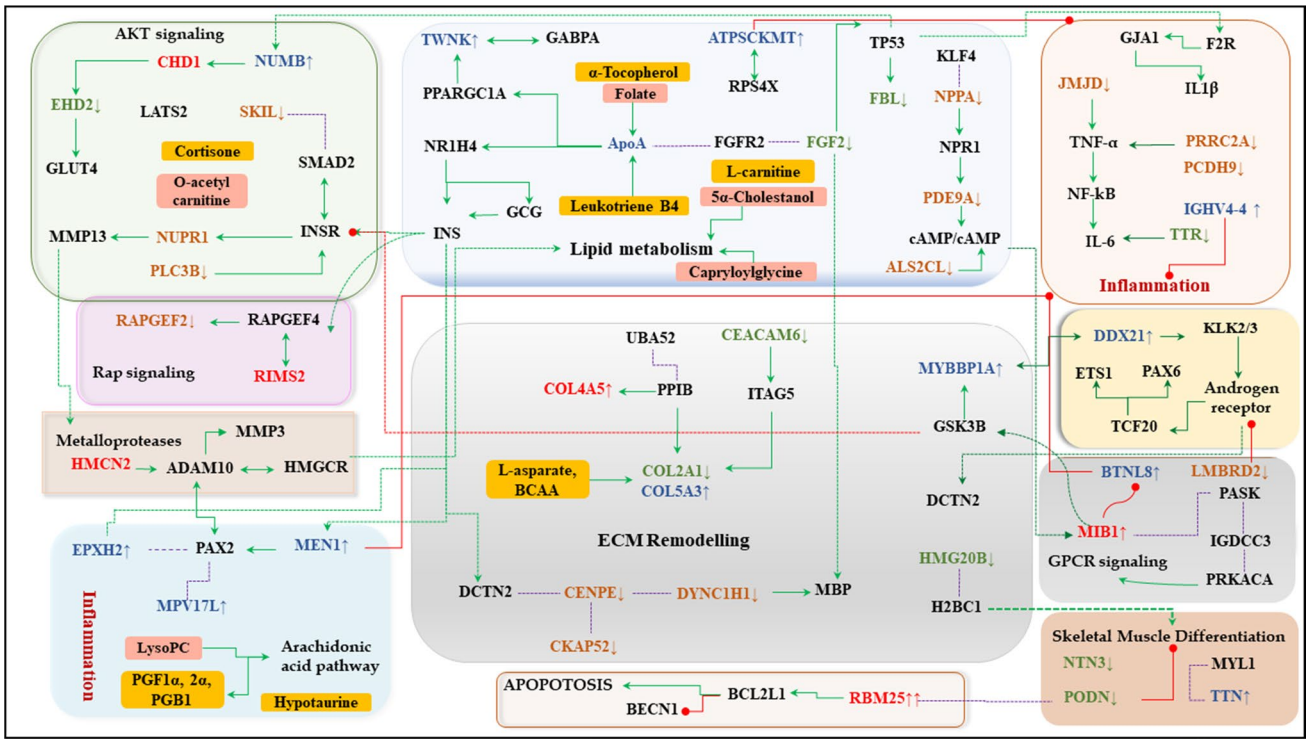

Fig. 6 Mechanism of action of TCE to regulate TG levels and secondary disorders in HTG patients explored from metabolomics and proteomics profiles. ● indicate protein up regulated in HLT; ● indicate protein downregulated in HLT; ● indicate protein up regulated in HTG_T; ● indicate protein down regulated in HTG_T; ⟷ indicate co-activation; → indicate activation; ····· indicate binding

berberine to increase APOA1 expression [49]. Increased levels of APOA1 and decreased levels of VLDL, and TG conferred the risk of atherosclerosis [50]. The current study provides the first practical evidence that TCE increased INSR and APOA1 expression. Drugs that increase APOA1 expression or ApoA1/ApoB ratio are found to be useful to HTG.

The present study accommodates certain lacuna of having a limited number of subjects that may induce certain errors in statistical analysis and limits the efficacy of TCE. Therefore, there is a need to investigate the potential of *T.cordifolia* with a large number of the individual to eliminate the chances of statistical error. It will be helpful towards the development of herbal therapeutics aid against hypertriglyceridemia as well as other associated disease conditions like pancreatitis, CVDs, and hypoxia. Primary as well as secondary outcomes from the biochemistry analysis and omics data suggested that TCE supplementation efficiently controlled the hypertriglyceridemia and associated complications in the patients.

Abbreviations HTG: Hypertriglyceridemia; TCE: Water extract of *T. cordifolia*; PPAR: Peroxisome proliferator-activated receptors; PLS-DA: Partial Least Square Discriminant Analysis; HPLC: High-Performance Liquid Chromatography; ESI-QTOF-MS: Electrospray Ionization Quadrupole Time of Flight Mass Spectrometry; *AST*: *Aspartate transaminase*; ALT: Alanine transaminase.

Supplementary Information The online version contains supplementary material available at https://doi.org/10.1007/s40200-022-00985-6.

Acknowledgements Authors wish to acknowledge the CCRAS, Ministry of AYUSH, Govt of India for supporting the work.

Author's contributions AS, AN and RD design the study and conducted the experiment. AY analysed the data and drafted the manuscript. JP and RD assisted in drafting the manuscript.

Data availability The data that support the findings of this study are available from the corresponding author upon reasonable request.

Declarations

Ethics approval Human Ethics Committee of the PDDYP Ayurveda College, Pune, India approved the study wide letter no. RRI/2011/HEC/2023 dated 18-02-2011.

Conflict of interest All authors declare that they have no conflict of interest.

References

1. Packard CJ, Boren J, Taskinen MR. Causes and consequences of hypertriglyceridemia. Front Endocrinol. 2020;11:252.
2. Ewald N. Hypertriglyceridemia-induced acute pancreatitis. Clin Lipidol. 2013;8:587–94.
3. Jialal I, Devaraj S (2019) Potential implications of redefining the hypertriglyceridemia of metabolic syndrome. Hormone Mol Biol Clin Investig.
4. Subramanian S, Chait A. Hypertriglyceridemia secondary to obesity and diabetes. Biochim Biophys Acta Mol Cell Biol Lipids. 2012;1821:819–25.
5. de Pretis N, Amodio A, Frulloni L. Hypertriglyceridemic pancreatitis: epidemiology, pathophysiology and clinical management. United European Gastroenterol J. 2018;6:649–55.
6. Ormazabal V, Nair S, Elfeky O, et al. Association between insulin resistance and the development of cardiovascular disease. Cardiovasc Diabetol. 2018;17:1–14.
7. Sahebkar A, Simental-Mendía LE, Watts GF, et al. Comparison of the effects of fibrates versus statins on plasma lipoprotein(a) concentrations: a systematic review and meta-analysis of head-to-head randomized controlled trials. BMC Med. 2017. https://doi.org/10.1186/s12916-017-0787-7.
8. Fruchart JC. Selective peroxisome proliferator-activated receptorα modulators (SPPARMα): the next generation of peroxisome proliferator-activated receptor α-agonists. Cardiovasc Diabetol. 2013;12:1–8.
9. Das UN. Bioactive lipids as mediators of the beneficial actions of statins. J Cardiovasc Pharmacol. 2019;74:4–8.
10. Sharma B, Yadav A, Dabur R. Interactions of a medicinal climber Tinospora cordifolia with supportive interspecific plants trigger the modulation in its secondary metabolic profiles. Sci Rep. 2019;9:1–16. https://doi.org/10.1038/s41598-019-50801-0.
11. Barter PJ, Rye KA. Cholesteryl ester transfer protein inhibition as a strategy to reduce cardiovascular risk. J Lipid Res. 2012;53:1755–66.
12. Singh D, Chaudhuri PK (2017) Chemistry and pharmacology of Tinospora cordifolia. In: Natural Product Communications. pp 299–308.
13. Patgiri B, Umretia B, Vaishnav P, et al. Anti-inflammatory activity of Guduchi Ghana (aqueous extract of Tinospora Cordifolia Miers.). AYU (An International Quarterly Journal of Research in Ayurveda). 2014;35:–108. https://doi.org/10.4103/0974-8520.141958.
14. Sharma U, Bala M, Kumar N, et al. Immunomodulatory active compounds from Tinospora cordifolia. J Ethnopharmacol. 2012;141:918–26. https://doi.org/10.1016/j.jep.2012.03.027.
15. Sharma R, Amin H, Galib, Prajapati PK. Antidiabetic claims of Tinospora cordifolia (Willd.) Miers: critical appraisal and role in therapy. Asian Pac J Trop Biomed. 2015;5:68–78.
16. Sannegowda KM, Venkatesha SH, Moudgil KD. Tinospora cordifolia inhibits autoimmune arthritis by regulating key immune mediators of inflammation and bone damage. Int J Immunopathol Pharmacol. 2015. https://doi.org/10.1177/0394632015608248.
17. Shirolkar A, Sharma B, Lata S, Dabur R. Guduchi Sawras (Tinospora cordifolia): An Ayurvedic drug treatment modulates the impaired lipid metabolism in alcoholics through dopaminergic neurotransmission and anti-oxidant defense system. Biomed Pharmacother. 2016;83:1265–77. https://doi.org/10.1016/j.biopha.2016.08.051.
18. Koppen LM, Whitaker A, Rosene A, Beckett RD. Efficacy of Berberine alone and in combination for the treatment of hyperlipidemia: a systematic review. J Evid-Based Complement Alternat Med. 2017;22:956–68.
19. Singh N, Sharma B. Toxicological effects of berberine and sanguinarine. Front Mol Biosci. 2018;5:21.
20. Shirolkar A, Gahlaut A, Hooda V, Dabur R. Phytochemical composition changes in untreated stem juice of Tinospora cordifolia (W) Mier during refrigerated storage. J Pharm Res. 2013;7:1–6. https://doi.org/10.1016/j.jopr.2013.01.018.
21. Klempfner R, Erez A, Sagit BZ, et al. Elevated triglyceride level is independently associated with increased all-cause mortality in patients with established coronary heart disease: twenty-two-year follow-up of the Bezafibrate infarction prevention study and registry. Circulation: Cardiovascular Quality and Outcomes. 2016. https://doi.org/10.1161/CIRCOUTCOMES.115.002104.
22. Corrado MJ, Kovacevic MP, Dube KM, et al. The incidence of Propofol-induced hypertriglyceridemia and identification of associated risk factors. Crit Care Explor. 2020. https://doi.org/10.1097/cce.0000000000000282.
23. Chernushevich IV, Loboda AV, Thomson BA. An introduction to quadrupole-time-of-flight mass spectrometry. J Mass Spectrom. 2001;36:849–65. https://doi.org/10.1002/jms.207.
24. Gromova I, Celis JE (2006) Protein Detection in Gels by Silver Staining: A Procedure Compatible with Mass Spectrometry. In: Cell Biology, Four-Volume Set. pp 219–223.
25. Sun X, Liu J, Wang G. Fenofibrate decreased microalbuminuria in the type 2 diabetes patients with hypertriglyceridemia. Lipids Health Dis. 2020. https://doi.org/10.1186/s12944-020-01254-2.
26. Shirolkar A, Yadav A, Mandal TK, Dabur R. Intervention of Ayurvedic drug Tinospora cordifolia attenuates the metabolic alterations in hypertriglyceridemia: a pilot clinical trial. J Diabetes Metab Disord. 2020. https://doi.org/10.1007/s40200-020-00657-3.
27. Kim M, Yoo HJ, Ko J, Lee JH. Metabolically unhealthy overweight individuals have high lysophosphatide levels, phospholipase activity, and oxidative stress. Clin Nutr. 2020. https://doi.org/10.1016/j.clnu.2019.04.025.
28. Lei P, Bai T, Sun Y. Mechanisms of ferroptosis and relations with regulated cell death: a review. Front Physiol. 2019. https://doi.org/10.3389/fphys.2019.00139.
29. Grygiel-Górniak B. Peroxisome proliferator-activated receptors and their ligands: nutritional and clinical implications - a review. Nutr J. 2014. https://doi.org/10.1186/1475-2891-13-17.
30. Chiang JYL, Li T (2009) Regulation of bile acid and cholesterol metabolism by PPARs. PPAR Res.
31. Weissglas-Volkov D, Pajukanta P. Genetic causes of high and low serum HDL-cholesterol. J Lipid Res. 2010;51:2032–57.
32. Friso S, Girelli D, Martinelli N, et al. Low plasma vitamin B-6 concentrations and modulation of coronary artery disease risk. Am J Clin Nutr. 2004;79:992–8. https://doi.org/10.1093/ajcn/79.6.992.
33. Mitu O, Cirneala IA, Lupsan AI, et al (2020) The effect of vitamin supplementation on subclinical atherosclerosis in patients without manifest cardiovascular diseases: never-ending Hope or underestimated effect? Molecules 25.
34. Vaidya A, Brown JM, Williams JS. The renin-angiotensin-aldosterone system and calcium-regulatory hormones. J Hum Hypertens. 2015;29:515–21.
35. Francis SH, Busch JL, Corbin JD. cGMP-dependent protein kinases and cGMP phosphodiesterases in nitric oxide and cGMP action. Pharmacol Rev. 2010;62:525–63.
36. Wijnker PJM, Sequeira V, DiWD K, Van Der Velden J. Hypertrophic cardiomyopathy: a vicious cycle triggered by sarcomere mutations and secondary disease hits. Antioxid Redox Signal. 2019;31:318–58.
37. Nakamura M, Sadoshima J. Mechanisms of physiological and pathological cardiac hypertrophy. Nat Rev Cardiol. 2018;15:387–407.
38. Pirinen E, Kuulasmaa T, Pietilä M, et al. Enhanced polyamine catabolism alters homeostatic control of white adipose tissue

mass, energy expenditure, and glucose metabolism. Mol Cell Biol. 2007. https://doi.org/10.1128/mcb.02034-06.
39. Pirinen E, Gylling H, Itkonen P, et al (2010) Activated polyamine catabolism leads to low cholesterol levels by enhancing bile acid synthesis. In: Amino Acids. pp 549–560.
40. Boucher J, Kleinridders A, Ronald Kahn C. Insulin receptor signaling in normal and insulin-resistant states. Cold Spring Harb Perspect Biol. 2014. https://doi.org/10.1101/cshperspect.a009191.
41. Luu BE, Zhang Y, Storey KB. The regulation of Akt and FoxO transcription factors during dehydration in the African clawed frog (Xenopus laevis). Cell Stress Chaperones. 2020. https://doi.org/10.1007/s12192-020-01123-y.
42. Moseti D, Regassa A, Kim WK. Molecular regulation of adipogenesis and potential anti-adipogenic bioactive molecules. Int J Mol Sci. 2016;17:124.
43. Fruman DA, Chiu H, Hopkins BD, et al. The PI3K pathway in human disease. Cell. 2017;170:605–35.
44. Campa CC, Ciraolo E, Ghigo A, et al. Crossroads of PI3K and Rac pathways. Small GTPases. 2015. https://doi.org/10.4161/21541248.2014.989789.
45. Gaonach-Lovejoy V, Boscher C, Delisle C, Gratton J-P. Rap1 is involved in Angiopoietin-1-induced cell-cell junction stabilization and endothelial cell sprouting. Cells. 2020;9:155. https://doi.org/10.3390/cells9010155.
46. Xiao H, Gu Z, Wang G, Zhao T. The possible mechanisms underlying the impairment of hif-1α pathway signaling in hyperglycemia and the beneficial effects of certain therapies. Int J Med Sci. 2013;10:1412–21.
47. Rye KA, Barter PJ, Cochran BJ. Apolipoprotein A-I interactions with insulin secretion and production. Curr Opin Lipidol. 2016;27:8–13.
48. Cochran BJ, Bisoendial RJ, Hou L, et al. Apolipoprotein A-I increases insulin secretion and production from pancreatic β-cells via a G-protein-cAMPPKA-FoxO1-dependent mechanism. Arterioscler Thromb Vasc Biol. 2014. https://doi.org/10.1161/ATVBAHA.114.304131.
49. Tan W, Wang Y, Wang K, et al. Improvement of endothelial dysfunction of Berberine in atherosclerotic mice and mechanism exploring through TMT-based proteomics. Oxidative Med Cell Longev. 2020;2020:8683404. https://doi.org/10.1155/2020/8683404.
50. Haghikia A, Landmesser U. Lipoproteins and cardiovascular redox signaling: role in atherosclerosis and coronary disease. Antioxid Redox Signal. 2018;29:337–52.
51. Armitage J, Holmes MV, Preiss D. Cholesteryl Ester transfer protein inhibition for preventing cardiovascular events: JACC review topic of the week. J Am Coll Cardiol. 2019;73:477–87.
52. Sharma P, Dwivedee BP, Bisht D, et al. The chemical constituents and diverse pharmacological importance of Tinospora cordifolia. Heliyon. 2019;5:e02437.
53. Woller SA, Choi SH, An EJ, et al. Inhibition of Neuroinflammation by AIBP: spinal effects upon facilitated pain states. Cell Rep. 2018;23:2667–77. https://doi.org/10.1016/j.celrep.2018.04.110.
54. Nagao K, Tomioka M, Ueda K. Function and regulation of ABCA1 - membrane meso-domain organization and reorganization. FEBS J. 2011;278:3190–203.